Supplementary Figure 1

a

MDYKDHDGDYKDHDIDYKDD
DDKMAPKKKRKVGIHGVPAA
MAERPFQCRICMRKFAQSGD
LTRHTKIHTGEKPFQCRICM
RNFSRSDVLSEHIRTHTGEK
PFACDICGKKFADRSNRIKH
TKIHTGSQKPFQCRICMRNF
SRSDNLSEHIRTHTGEKPFA
CDICGRKFAQNATRINHTKI
HLRGSQLVKSELEEKKSELR
HKLKYVPHEYIELIEIARNS
TQDRILEMKVMEFFMKVYGY
RGKHLGGSRKPDGAIYTVGS
PIDYGVIVDTKAYSGGYNLP
IGQADEMERYVEENQTRNKH
LNPNEWWKVYPSSVTEFKFL
FVSGHFKGNYKAQLTRLNHI
TNCNGAVLSVEELLIGGEMI
KAGTLTLEEVRRKFNNGEIN
F

b

MDYKDHDGDYKDHDIDYKDD
DDKMAPKKKRKVGIHGVPER
PFQCQICMRNFSRSDSLSVH
IRTHTGEKPFACDICGRKFA
TSGHLSRHTKIHTGSQKPFQ
CRICMRNFSRSDHLSQHIRT
HTGEKPFACDICGRKFAHAS
TRHCHTKIHLRGSQLVKSEL
EEKKSELRHKLKYVPHEYIE
LIEIARNSTQDRILEMKVME
FFMKVYGYRGKHLGGSRKPD
GAIYTVGSPIDYGVIVDTKA
YSGGYNLPIGQADEMQRYVK
ENQTRNKHINPNEWWKVYPS
SVTEFKFLFVSGHFKGNYKA
QLTRLNHKTNCNGAVLSVEE
LLIGGEMIKAGTLTLEEVRR
KFNNGEINF

Supplementary Figure 1 - F9 ZFN pair amino acid sequence.
Amino acid sequence of FLAG-tagged **a**, left F9 ZFN and **b,** right F9 ZFN.

Supplementary Figure 2

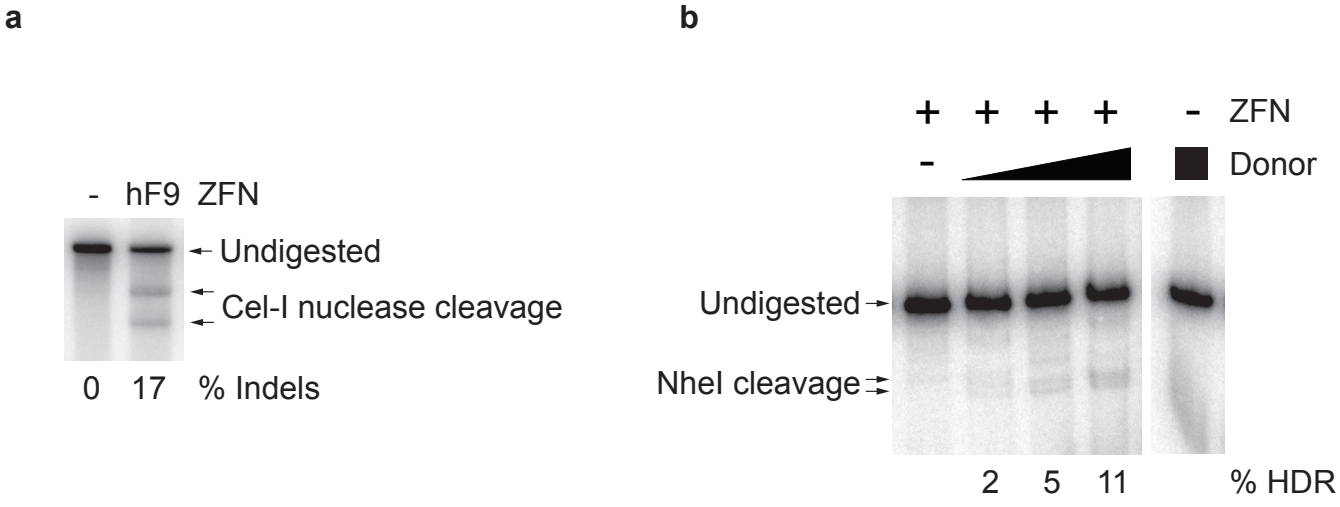

Supplementary Figure 2 - F9 ZFNs cleave human *F9* intron 1 and induce homology-directed repair in Hep3B cells.
a, Transfection of 400 ng of ZFN expression plasmid into Hep3B cells results in cleavage of the human *F9* intron 1 at day 3 post-transfection. Cel-1 assay performed with PCR using ^{32}P-labeled nucleotides, followed by PAGE and band intensity quantification by autoradiography. **b,** Co-transfection of 400 ng of ZFN expression plasmid with increasing amounts of NheI donor plasmid (0, 1, 2, and 4 μg) results in increasing levels of HDR at days 3 post-transfection, whereas transfection of the NheI donor alone (4 μg) does not result in detectable HDR. HDR PCR performed with PCR using ^{32}P-labeled nucleotides, followed by PAGE and band intensity quantification by autoradiography. Lanes with no quantification had no detectable HDR.

Supplementary Figure 3

a

b

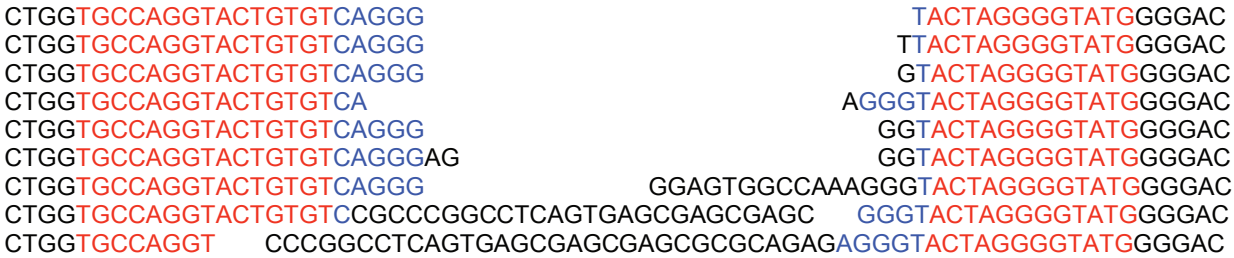

Supplementary Figure 3 - Sequencing of target site insertions and deletions induced by ZFNs *in vivo*. PCR products from Cel-1 assay on ZFN-treated mice in Fig.2c were cloned and sequenced prior to treatment with Cel-1 enzyme. Sequencing of clones demonstrated **a**, deletions and **b**, insertions characteristic of imprecise DSB repair by NHEJ. Red bases indicate ZFN binding sites while blue bases indicate the 6 bp regionof ZFN cleavage. Intervening white regions represent deleted bases while black bases in between ZFN binding sites indicate inserted bases. The 5' and 3' flanking black bases indicate hF9mut intron. The top line of each panel indicates the sequence of the unmodified locus.

Supplementary Figure 4

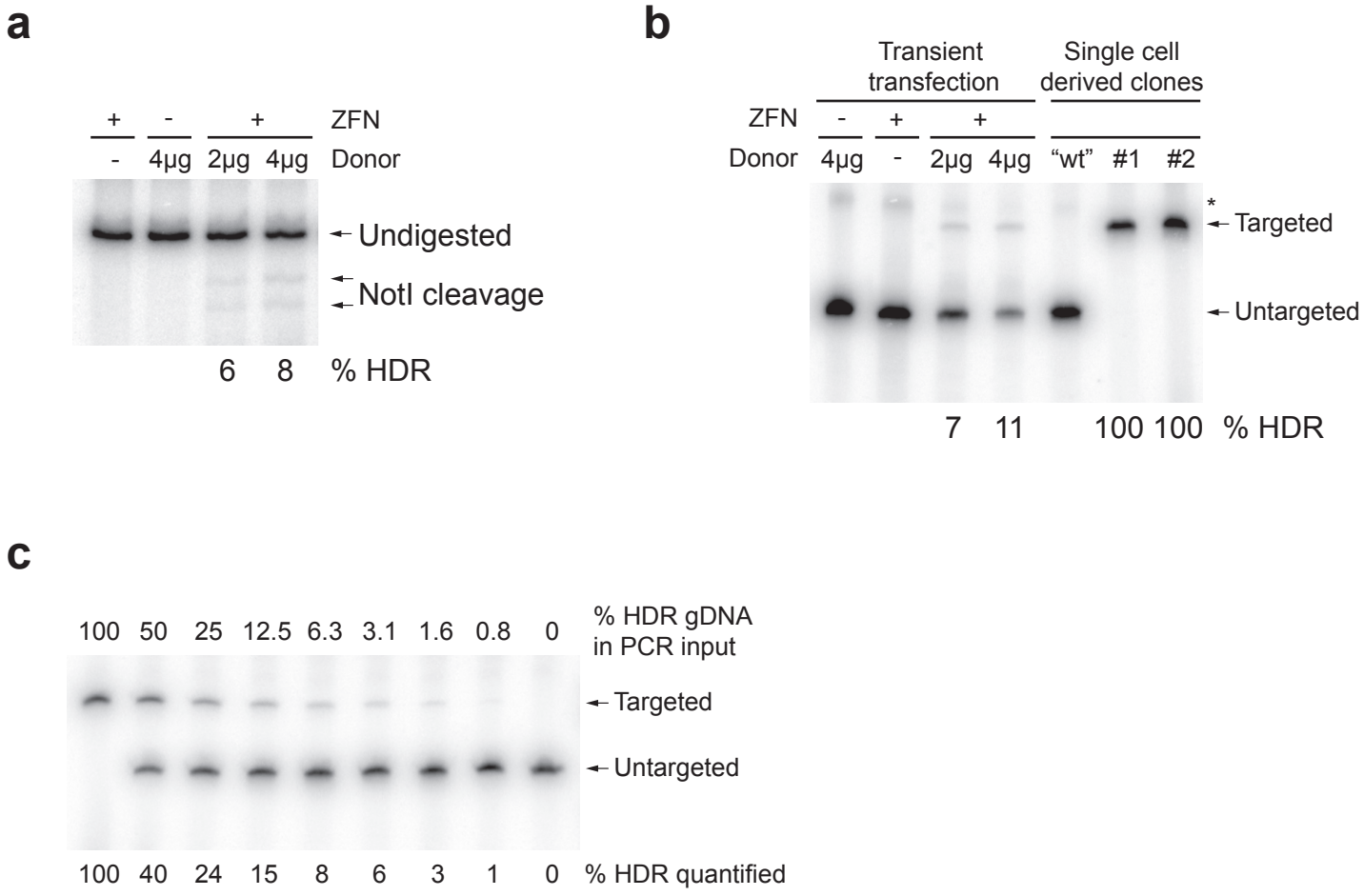

Supplementary Figure 4 - F9 ZFNs promote HDR at the h*F9*mut intron in HEK293T-h*F9*mut cells and HDR can be quantified through PCR.

HEK293T cells were stably transduced with a lentiviral vector carrying the h*F9*mut mini-gene and a single cell-derived clone was expanded. **a,** Co-transfection of HEK293T-h*F9*mut cells with 400 ng of ZFN expression plasmid and 2 µg or 4 µg of NotI RFLP donor plasmid results in gene targeting 3 days post-transfection, whereas transfection of 400 ng of ZFN expression plasmid alone, or 4 µg of donor plasmid does not result in detectable HDR. **b,** Targeted integration of the "splice acceptor – exons 2-8 coding sequence – bovine growth hormone polyA signal" cassette in HEK293T-h*F9*mut cells followed by the isolation of either untargeted ("wt") or targeted single cell-derived clones (#1 and #2). (*) denotes non-specific amplicon present in all samples. **c,** Linearity of the PCR-based quantitative detection of HDR using primers P1/P3. Genomic DNA isolated from a single cell-derived targeted clone (#1) was mixed at various ratios with wild-type (non-targeted) gDNA and amplified by PCR using ^{32}P-labeled nucleotides followed by PAGE and autoradiography. The intensity of the non-targeted and targeted bands were quantified. The % of detected targeted signal is shown below the gel and the theoretical signal is shown above.

Supplementary Figure 5

a

Week of life	ZFN+Donor	Mock+Donor	ZFN Alone	p-value
	h*F9*mut average plasma hF.IX, ng/mL (n, std. dev.)			
4	124 (7, 117)	≤15 (6, 0)	≤15 (7, 0)	0.003
6	119 (7, 111)	≤15 (6, 0)	≤15 (7, 0)	0.003
8	119 (7, 122)	≤15 (6, 0)	≤15 (7, 0)	0.006
10 wks 1 day	156 (7, 140)	≤15 (6, 0)	≤15 (7, 0)	0.002
10 wks 2 days	205 (7, 170)	≤15 (6, 0)	≤15 (7, 0)	0.0006
11	156 (7, 149)	≤15 (6, 0)	≤15 (7, 0)	0.003
12	171 (7, 165)	16 (6, 1)	≤15 (7, 0)	0.003
13	126 (7, 123)	≤15 (6, 0)	≤15 (7, 0)	0.004
14	121 (7, 116)	≤15 (6, 0)	≤15 (7, 0)	0.003
16	176 (7, 144)	≤15 (6, 0)	≤15 (7, 0)	0.0006
18	177 (7, 136)	≤15 (6, 0)	≤15 (7, 0)	0.003
22	137 (7, 133)	≤15 (6, 0)	≤15 (6, 0)	0.003
32	189 (7, 223)	≤15 (6, 0)	17 (7, 4)	0.01

b

Week of life	ZFN+Donor	Mock+Donor	p-value
	h*F9*mut/HB average plasma hF.IX, ng/mL (n, std. dev.)		
4	262 (9, 96)	24 (9, 17)	0.000006
6	354 (8, 183)	21 (8, 10)	0.0001
8	217 (6, 160)	18 (4, 7)	0.04
12	256 (5, 86)	16 (3, 2)	0.003
13	166 (5, 38)	15 (3, 0)	0.0006
14	284 (5, 49)	18 (3, 6)	0.0001

Supplementary Figure 5 - Significant difference in hF.IX expression between groups.

a, hF.IX expression in ZFN+Donor group at multiple time-points compared to ZFN alone and Mock+Donor groups in h*F9*mut mice from Figure 4a. p-values from 2-tailed T-test.

b, hF.IX expression in ZFN+Donor group at multiple time-points compared to Mock+ Donor group in h*F9*mut/HB mice from Figure 5a. p-values from 2-tailed T-test.

Supplementary Figure 6

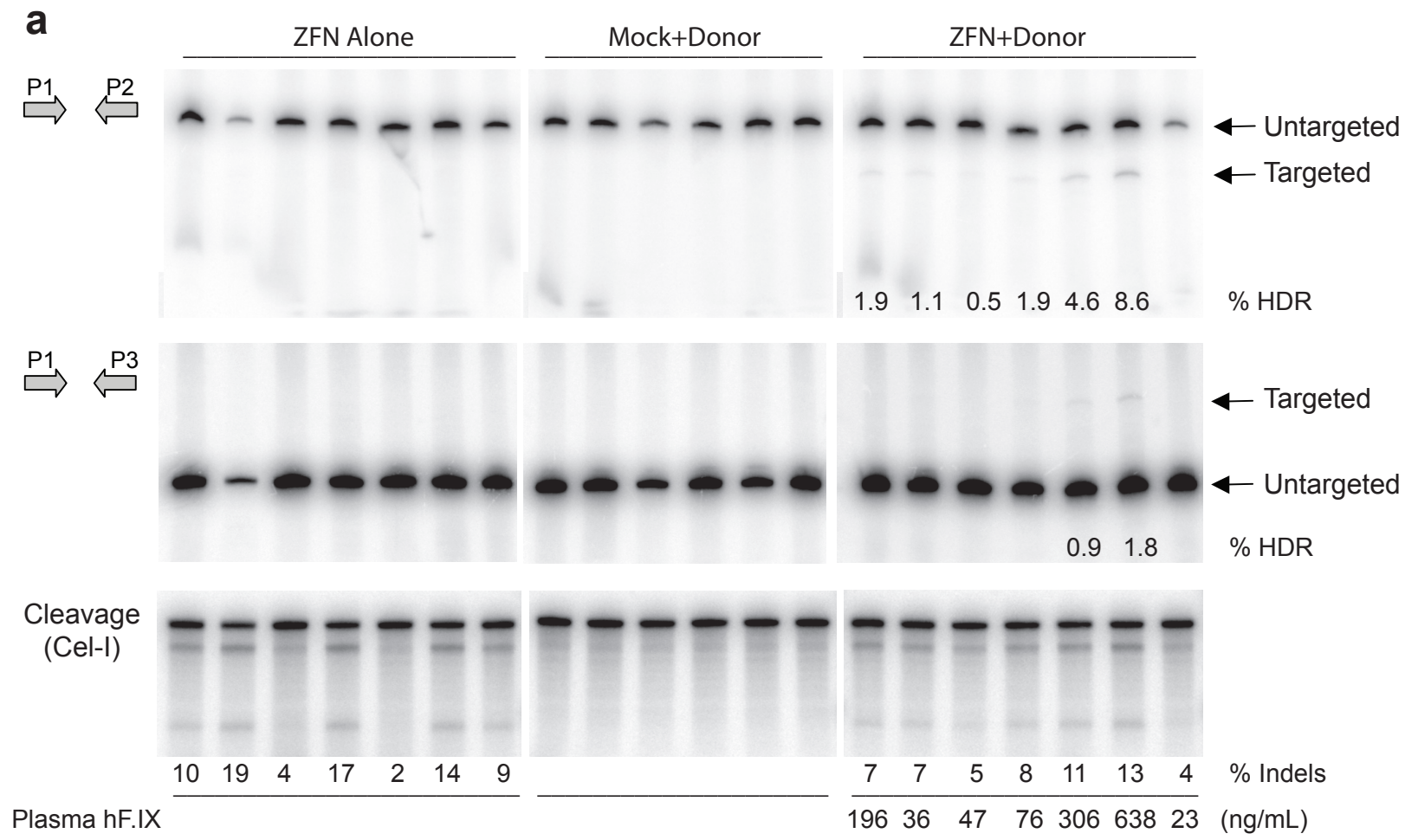

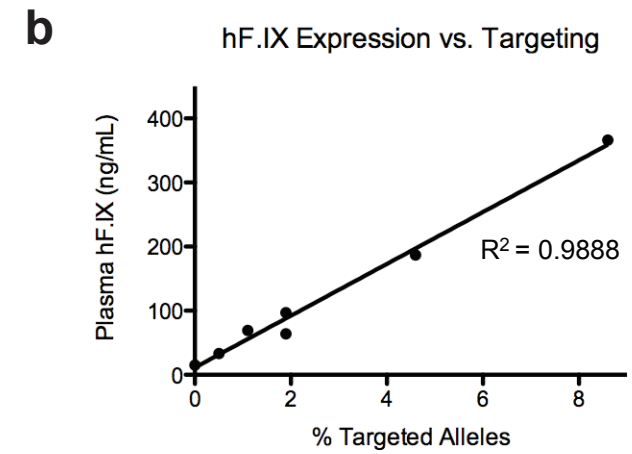

Supplementary Figure 6 - Correlation of ZFN activity, HDR efficiency, and hF.IX expression in hF9mut mice.

a, Quantification of HDR efficiency using primers P1/P2 and P1/P3 PCR assays, quantification of ZFN-induced indel frequency using the Cel-I assay, and measurement of plasma hF.IX levels by ELISA in mice from Fig.4a at 32 weeks of life demonstrates correlation of ZFN cleavage activity with HDR efficiency and hF.IX expression. PCR was performed using ^{32}P-labeled nucleotides, followed by PAGE and product band intensity quantification by autoradiography. Lanes with no quantification were below the limit of detection. Each lane represents an individual mouse. **b,** Linear regression of plasma hF.IX versus HDR targeting rate, as measured using primers P1/P2, demonstrates association between degree of HDR and level of hF.IX expression.

Supplementary Figure 7

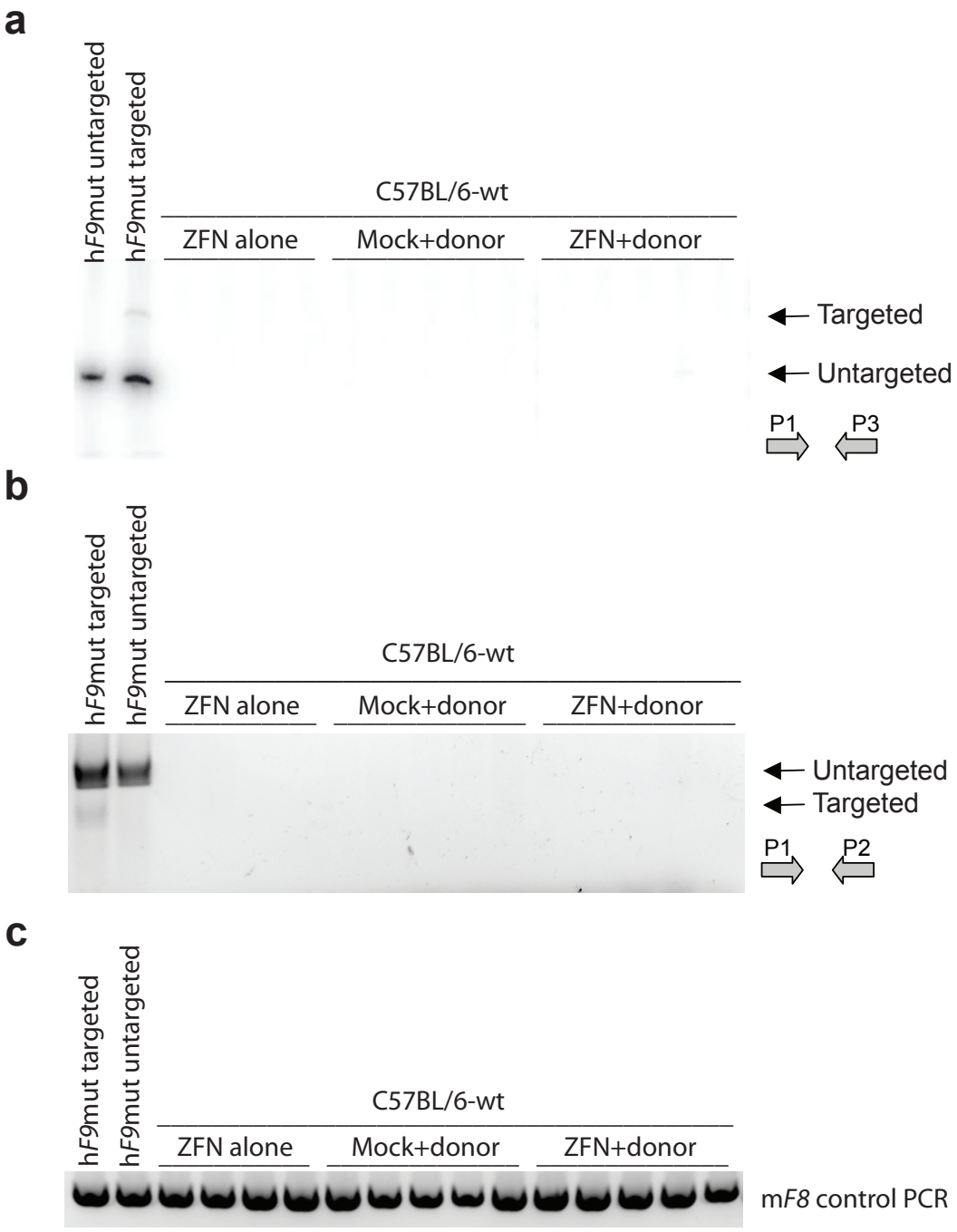

Supplementary Figure 7 - Lack of amplification products for PCR-based HDR quantification assays in C57BL/6-wt mice.
Liver genomic DNA from control mice in Fig.4c was PCR amplified using **a**, primers P1/P3, **b**, primers P1/P2, or **c**, endogenous mouse F8 gene (to show no inhibition of PCR) primers. PCR was performed using ^{32}P-labeled nucleotides, followed by PAGE and product band detection by **a**, autoradiography, or **b-c**, ethidium bromide staining. Each lane represents an individual mouse.

Supplementary Figure 8

a

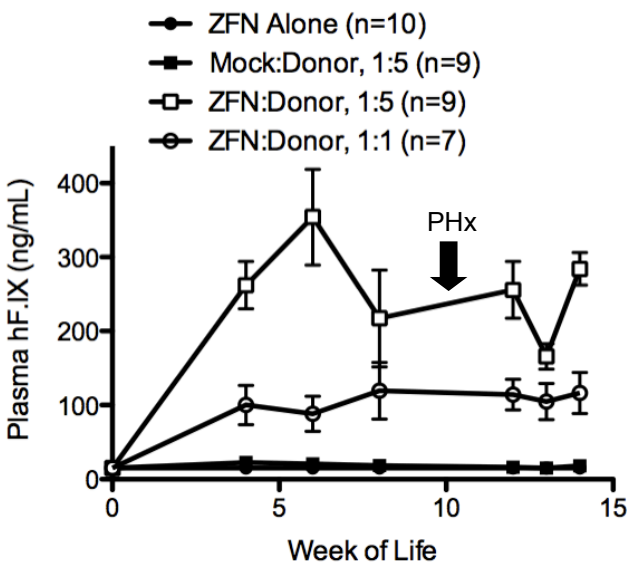

b

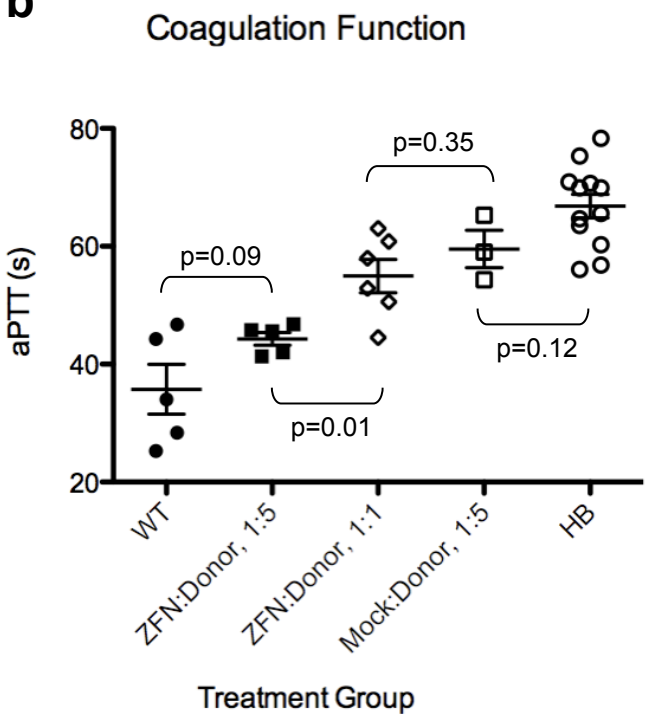

c

Week of life	ZFN:Donor, 1:5	ZFN:Donor, 1:1	p-value
	hF9mut/HB average plasma hF.IX, ng/mL (n, std. dev.)		
4	262 (9, 96)	100 (7, 70)	0.002
6	354 (8, 183)	88 (7, 63)	0.003
8	217 (6, 160)	119 (7, 101)	0.2
12	256 (5, 86)	98 (6, 58)	0.005
13	166 (5, 38)	105 (6, 60)	0.08
14	284 (5, 49)	116 (6, 68)	0.001

Supplementary Figure 8 - hF.IX expression and aPTT correction are dependent on Donor dose.

a, Plasma hF.IX in h*F9*mut/HB mice following day 2 of life I.P. injection with ZFN alone (5e10vg), Mock(5e10vg)+Donor(2.5e11vg), ZFN(5e10vg)+Donor(2.5e11vg), or ZFN (5e10vg)+Donor(5e10vg). Error bars denote std. error. PHx=partial hepatectomy.

b, Test of clot formation by aPTT at week 14 of life for mice from panel a as well as WT and HB control mice. p-values from 2-tailed T-test.

c, hF.IX expression in ZFN:Donor, 1:5 group at multiple time-points compared to ZFN:Donor, 1:1 group in h*F9*mut/HB mice. p-values from 2-tailed T-test.

Supplementary Figure 9

Predicted ZFN target site

gTGCCAGGTACTGTGTcagggtACTAGGGGTCTGg
(Left ZFN) (Right ZFN)

Chr.	Location	Nucleotide position (mm8 build)	Potential site	Mismatches*	Gene	Position in Gene	Cel-1 (%)
chr9	9qE3.1	85644480-85644514	AaGgCAGGTgCTGTGTAAGTACACTAaGGaTGTGc	5	none	N/A	4
chr2	2qH4	178784182-178784212	TCACACCCtTAGGAAGAGAgTgGGGGTCTGG	3	none	N/A	<1
chr4	4qB3	58366981-58367014	CCgGACtCCTAGGACCCAgCACAGTgCCCGGCAC	4	none	N/A	<1
chr11	11qB4	71934573-71934603	CCACACCCtgAGGAGAAGCCTAGtGtTCTGG	4	Pitpnm3	Intron 2	<1
chrX	XqC3	95501151-95501184	ATGCCAtGTCCTGTGcCCTGTgCcAGGGaTGTGG	5	none	N/A	<1
chr14	14qA3	27637751-27637781	TCAaACCCCTAGGAAAATgCTAGaGGTCaGT	4	none	N/A	<1
chr4	4qD2.2	121711455-121711485	ACAtACtCtTAGGGTACTACTcaGGGTCTGG	5	none	N/A	<1
chr4	4qD2.2	121973087-121973117	ACAtACtCtTAGGGTACTACTcaGGGTCTGG	5	none	N/A	<1
chr5	5qF	120448948-120448978	TCACAgCCacAGGACCCCACTAGGGGTGTGG	3	Rbm19	Intron 23	<1
chr8	8qA1.1	12898527-12898558	CCgCACaCCTtaGGGAAAACCTAGGGGTCTGG	4	none	N/A	<1
chr2	2qB	35247904-35247934	CCcCACCCtcAGcAGCCTggTAGGGGTGTGT	6	Ggta1	Intron 2	<1
chr13	13qD1	97361947-97361977	AaACACCCCTAGGAGTCTCCTgGGGaTGgGG	4	none	N/A	<1
chr7	7qF3	125662683-125662713	CCACtCtCCTAGTGGAAGgCTAaGGGTCTGA	4	D430042O09Rik	Intron 24	<1
chr19	19qD1	50113440-50113470	TCACAtCCtTAGTAGCATCCTtaGaGTGTGG	5	none	N/A	<1
chr4	4qD3	136746026-136746056	CCAGctCCCTAGTGGCTTCCTAaaGGTCTGC	4	Hspg2	Intron 1	<1
chr4	4qD2.2	123884923-123884954	TCgCAaCCCTAGGCAGAGAgCcAGGGGTCTGG	4	none	N/A	<1
chr3	3qE3	79023411-79023441	CCtGACCCtTAGTAACCTgCTAatGtTCTGA	6	none	N/A	<1
chr1	1qA2	9983321-9983355	CCAGACCCtTAGGTCCGTAACACtGTAgCTGGgAG	4	Lrrc67	Intron 5	<1
chr4	4qB2	52798123-52798154	GCgCAtCCtTAGTAGTTGACCTAGGGGTCTtT	4	none	N/A	<1
chr7	7qD1	74726604-74726634	GCAGACCCCTtGTTCTGTgCTAGGGaTGgGG	4	none	N/A	<1

Supplementary Figure 9 - Off-target cleavage by F9 ZFNs *in vivo.*
Potential off-target cleavage sites in the mouse genome as determined using a SELEX approach. Mismatches are indicated by lower-case letters. To determine the frequency of off-target ZFN-induced insertions and deletions, the Cel-I assay was performed at each site using liver genomic DNA of mice from Figure 2c and averaged among the 4 samples.

Supplementary Figure 10

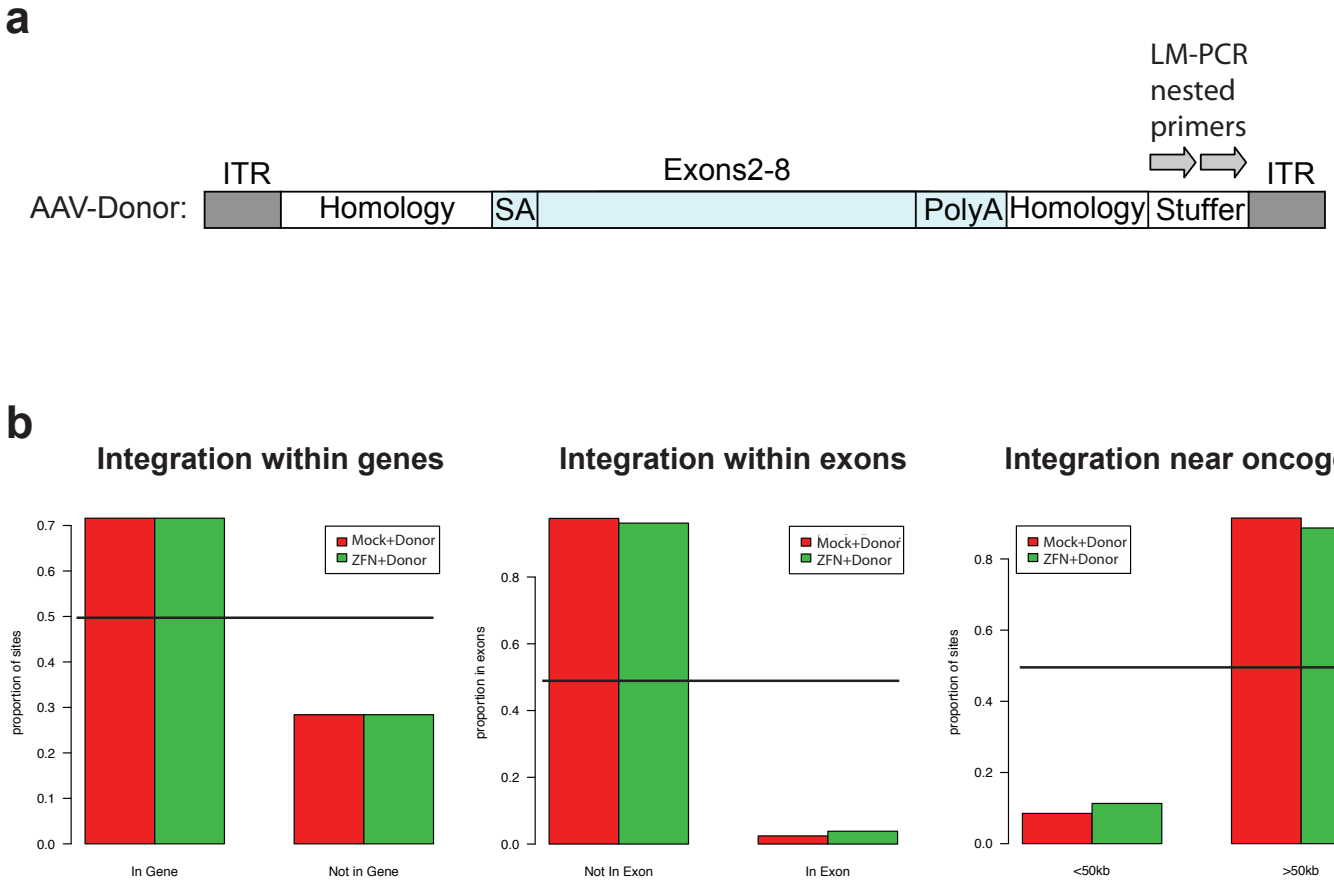

Supplementary Figure 10- LM-PCR cloning and 454 pyrosequencing to characterize AAV-F9 donor integration junctions at off-target sites.

We used the strategy described in Li et al., 2011 to characterize AAV-Donor integration sites in the mouse genome at sites distant from the h*F9* target site. **a,** LM-PCR strategy to clone NHEJ-mediated events by using donor vector primers hybridizing to the stuffer. The stuffer is outside the arms of homology and thus is eliminated by HDR events. This approach thus maps integration sites where the stuffer remained intact (i.e. NHEJ-dependent integrations) and could not query HDR-mediated events because 454 reads would not span the length of the arms of homology. To create the second primer binding site, genomic DNA was cleaved with a restriction enzyme and ligated to a linker, which was then used as the binding site for the reverse PCR primer. **b,** Integration site preferences for AAV Donor integrations within the mouse genome. One plate of 454/Roche Titanium sequencing was used to query integration sites from five mice treated with ZFN + Donor, and five control mice treated with Mock + Donor. The number of junction sequence reads aligning to unique sites in the mouse genome in each group were 5801 (ZFN + Donor) or 14048 (Mock + Donor). The relative likelihood of donor integrations to occur within genes, within exons, and within 50kb of oncogenes relative to randomly selected sites within the mouse genome[30] are indicated by the bar graphs (red for Mock + Donor and green for ZFN + Donor). Events are more likely to occur than random if above the black line and less likely if below the black line. No significant differences were detected in the presence or absence of the AAV-ZFN vector for these comparisons, indicating that ZFN cleavage at off-target sites did not have a strong effect on vector integration. Sequence data are available from the National Center for Biotechnology Information (NCBI) Genome Survey Sequences Database (GSSS, www.ncbi.nlm.nih.gov/dbGSS, accession numbers: HR941099 - HR999999, and JJ000001-JJ725186).

Supplementary Figure 11

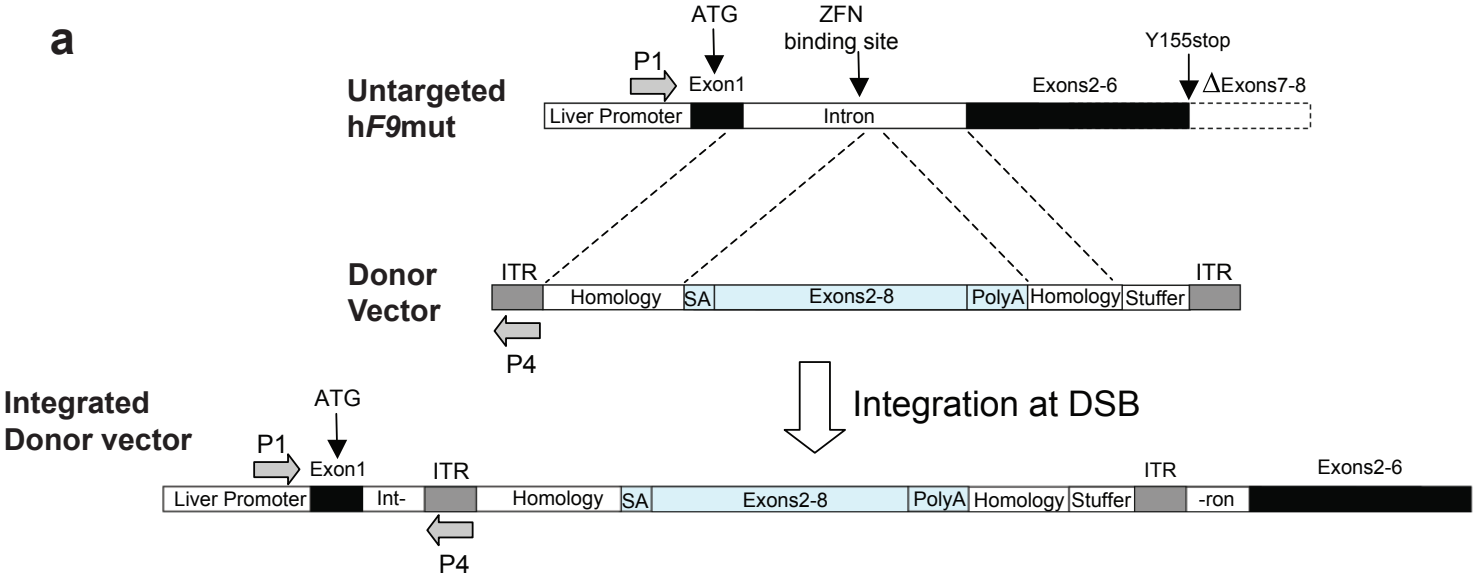

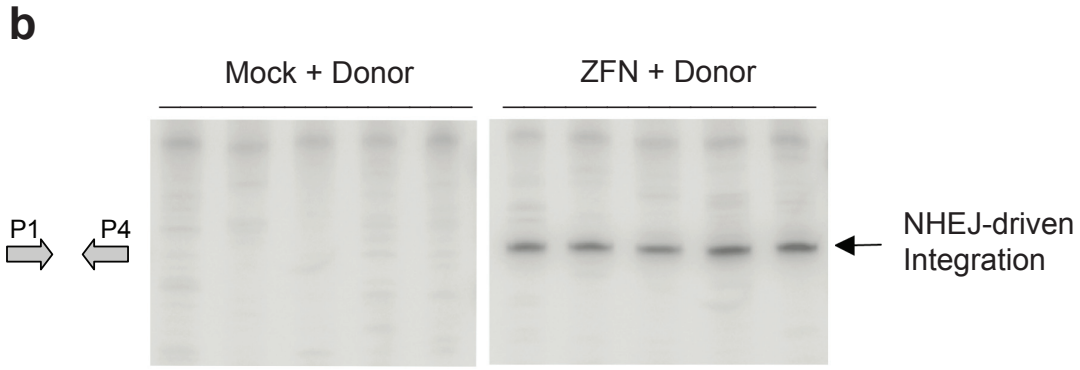

Supplementary Figure 11 - Capture of vector genome at the ZFN target site.
a, Vector DNA targeted integration at the ZFN target site can be detected through PCR using primers P1 and P4. **b,** PCR analysis with primer pair P1/P4 showing vector integration at the ZFN target site. PCR was performed using ^{32}P-labeled nucleotides, followed by PAGE and autoradiographed.

Supplementary Figure 12

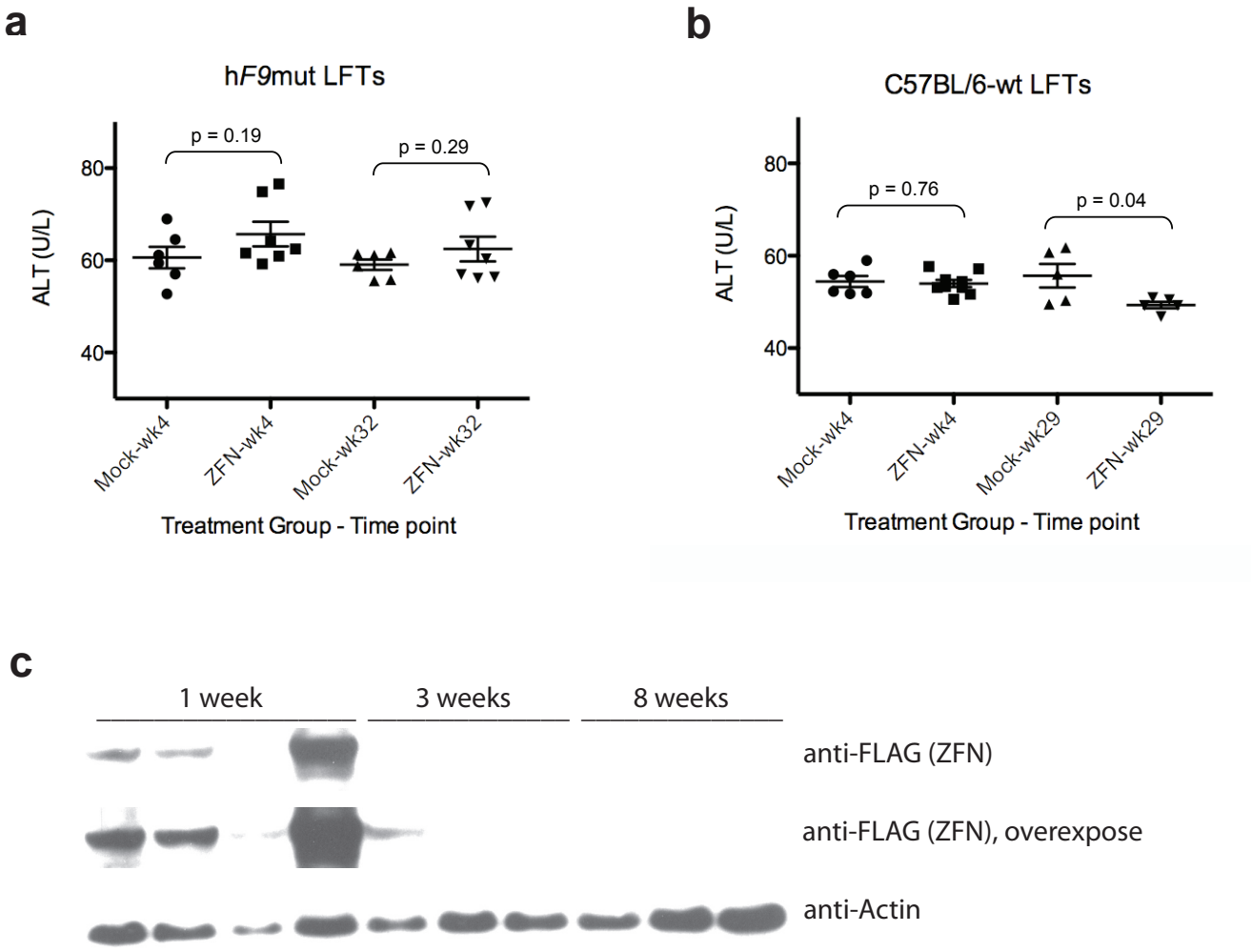

Supplementary Figure 12 - Kinetics of liver function tests and ZFN expression after neonatal injection. Measurement of plasma alanine aminotransferase (ALT) by chromogenic assay as a marker for liver damage at various time-points following day 2 of life I.P. injection of 2.5e11 v.g. AAV-Donor and 5e10 v.g. of AAV-ZFN or AAV-Mock in **a**, hF9mut and **b**, C57BL/6-wt mice. **c**, Western blotting to detect ZFN expression in whole liver lysate at weeks 1, 3, and 8 post- day 2 of life I.P. injection of 5e10 v.g. of AAV-ZFN. Note that the loss of ZFN expression by 3 weeks of life likely contributes to the absence of toxicity.

Supplementary Figure 13

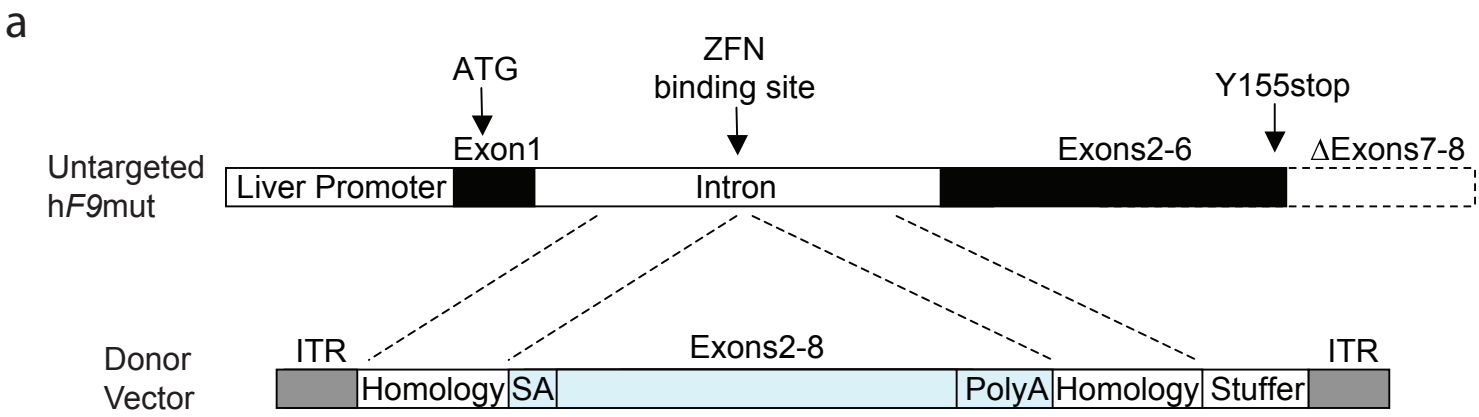

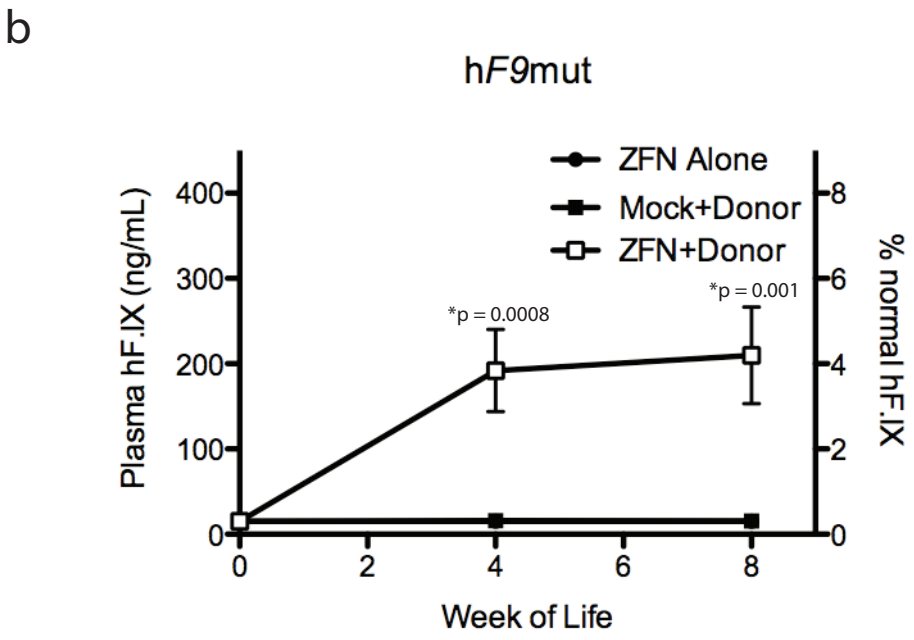

Supplementary Figure 13 - Expression of hF.IX in mice receiving ZFN and a Donor lacking exon 1 in the left arm of homology.

a, Schematic showing the map of a donor vector, distinct from the donor vector in Fig.3a in that it does not contain exon 1 sequence within the 5' arm of homology. **b**, Plasma hF.IX levels in hF9mut mice following I.P. injection at day 2 of life with either 5e10 v.g. AAV-ZFN alone (n=7), 5e10 v.g. AAV-ZFN and 2.5e11 v.g. of the new AAV-Donor (n=8), or 5e10 v.g. AAV-Mock and 2.5e11 v.g. of the new AAV-Donor (n=10). Plasma hF.IX assayed by ELISA. Error bars denote standard error. P-values from 2-tailed T-test.

Supplementary Figure 14

ATTTAAATGGCCGGCCAGTAGGCTCAGAGGCACACAGGAGTTTCTGGGCTCACCCTGCCCCCTTCCA
ACCCCTCAGTTCCCATCCTCCAGCAGCTGTTTGTGTGCTGCCTCTGAAGTCCACACTGAACAAACTTC
AGCCTACTCATGTCCCTAAAATGGGCAAACATTGCAAGCAGCAAACAGCAAACACACAGCCCTCCCTG
CCTGCTGACCTTGGAGCTGGGGCAGAGGTCAGAGACCTCTCTGGGCCCATGCCACCTCCAACATCCA
CTCGACCCCTTGGAATTTCGGTGGAGAGGAGCAGAGGTTGTCCTGGCGTGGTTTAGGTAGTGTGAGA
GGGGTACCCGGGGATCTTGCTACCAGTGGAACAGCCACTAAGGATTCTGCAGTGAGAGCAGAGGGC
CAGCTAAGTGGTACTCTCCCAGAGACTGTCTGACTCACGCCACCCCCTCCACCTTGGACACAGGACG
CTGTGGTTTCTGAGCCAGGTACAATGACTCCTTTCGGTAAGTGCAGTGGAAGCTGTACACTGCCCAGG
CAAAGCGTCCGGGCAGCGTAGGCGGGCGACTCAGATCCCAGCCAGTGGACTTAGCCCCTGTTTGCT
CCTCCGATAACTGGGGTGACCTTGGTTAATATTCACCAGCAGCCTCCCCCGTTGCCCCTCTGGATCCA
CTGCTTAAATACGGACGAGGACAGGGCCCTGTCTCCTCAGCTTCAGGCACCACCACTGACCTGGGAC
AGTGAATGATCCCCCTGATCTGCGGCCTCGACGGTATCGATAAGCTTGATATCGAATTCTAGTCGTCGA
CCACTTTCACAATCTGCTAGCAAAGGTTATGCAGCGCGTGAACATGATCATGGCAGAATCACCAGGCC
TCATCACCATCTGCCTTTTAGGATATCTACTCAGTGCTGAATGTACAGGTTTGTTTCCTTTTTTAAAATAC
ATTGAGTATGCTTGCCTTTTAGATATAGAAATATCTGATGCTGTCTTCTTCACTAAATTTTGATTACATGAT
TTGACAGCAATATTGAAGAGTCTAACAGCCAGCACGCAGGTTGGTAAGTACTGGTTCTTTGTTAGCTAG
GTTTTCTTCTTCTTCATTTTTAAAACTAAATAGATCGACAATGCTTATGATGCATTTATGTTTAATAAACACT
GTTCAGTTCATGATTTGGTCATGTAATTCCTGTTAGAAAACATTCATCTCCTTGGTTTAAAAAAATTAAAA
GTGGGAAAACAAAGAAATAGCAGAATATAGTGAAAAAAAATAACCACATTATTTTTGTTTGGACTTACCA
CTTTGAAATCAAAATGGGAAACAAAAGCACAAACAATGGCCTTATTTACACAAAAAGTCTGATTTTAAGA
TATATGACATTTCAAGGTTTCAGAAGTATGTAATGAGGTGTGTCTCTAATTTTTTAAATTATATATCTTCAAT
TTAAAGTTTTAGTTAAAACATAAAGATTAACCTTTCATTAGCAAGCTGTTAGTTATCACCAAAGCTTTTCAT
GGATTAGGAAAAAATCATTTTGTCTCTATGTCAAACATCTTGGAGTTGATATTTGGGGAAACACAATACT
CAGTTGAGTTCCCTAGGGGAGAAAAGCAAGCTTAAGAATTGACATAAAGAGTAGGAAGTTAGCTAATGC
AACATATATCACTTTGTTTTTTCACAACTACAGTGACTTTATGTATTTCCCAGAGGAAGGCATACAGGGA
AGAAATTATCCCATTTGGACAAACAGCATGTTCTCACAGGAAGCATTTATCACACTTACTTGTCAACTTT
CTAGAATCAAATCTAGTAGCTGACAGTACCAGGATCAGGGGTGCCAACCCTAAGCACCCCCAGAAAGC
TGACTGGCCCTGGTGCCAGGTACTGTGTCAGGGTACTAGGGGTATGGGGACAGGTTAGTCCACCTGA
GTGGGAAGAAGCGGTGAAAGGAGTCCAATCCATGTTTAAATGGCGGCAGTTGCAAGGAGCTGGTCAT
CCTCATCCTGATAAACTGCAAAAGGCTGCGGCAGTTACGCTAGGGATAACAGGGTAATATAGGGTGGTT
CCCACTCCAGACATGATGTCAGCTGTGAAATCGACGTCGCTGGACCATAATTAGGCTTCTGTTCTTCAG
GAGACATTTGTTCAAAGTCATTTGGGCAACCATATTCTGAAAACAGCCCAGCCAGGGTGATGGATCACT
TTGCAAAGATCCTCAATGAGCTATTTTCAAGTGATGACAAAGTGTGAAGTTAACCGCTCATTTGAGAAC
TTTCTTTTTCATCCAAAGTAAATTCAAATATGATTAGAAATCTGACCTTTTATTACTGGAATTCTCTTGACT
AAAAGTAAAATTGAATTTTAATTCCTAAATCTCCATGTGTATACAGTACTGTGGGAACATCACAGATTTTG
GCTCCATGCCCTAAAGAGAAATTGGCTTTCAGATTATTTGGATTAAAAACAAAGACTTTCTTAAGAGATG
TAAAATTTTCATGATGTTTTCTTTTTTGCTAAAACTAAAGAATTATTCTTTTACATTTCAGTTTTTCTTGATC
ATGAAAACGCCAACAAAATTCTGAATCGGCCAAAGAGGTATAATTCAGGTAAATTGGAAGAGTTTGTTC
AAGGGAACCTTGAGAGAGAATGTATGGAAGAAAAGTGTAGTTTTGAAGAAGCACGAGAAGTTTTTGAA
AACACTGAAAGAACAACTGAATTTTGGAAGCAGTATGTTGATGGAGATCAGTGTGAGTCCAATCCATGT
TTAAATGGCGGCAGTTGCAAGGATGACATTAATTCCTATGAATGTTGGTGTCCCTTTGGATTTGAAGGA
AAGAACTGTGAATTAGATGTAACATGTAACATTAAGAATGGCAGATGCGAGCAGTTTTGTAAAAATAGTG
CTGATAACAAGGTGGTTTGCTCCTGTACTGAGGGATATCGACTTGCAGAAAACCAGAAGTCCTGTGAA
CCAGCAGTGCCATTTCCATGTGGAAGAGTTTCTGTTTCACAAACTTCTAAGCTCACCCGTGCTGAGGC
TGTTTTTCCTGATGTGGACTATAGGGCCGGCCATTTAAAT

Supplementary Figure S14 - h*F9*mut mini-gene sequence.
Nucleotide sequence for the h*F9*mut construct. Underlined regions indicate liver enhancer and promoter (bases 20-742), h*F9* exon 1 (bases 808-923), ZFN target site (bases 1881-1910), and h*F9* exons 2-6 (bases 2548-3062).